

**Terreuspyridine: An Unexpected Pyridine Fused Meroterpenoid
Alkaloid with a Tetracyclic 6/6/6/6 Skeleton from *Aspergillus
terreus***

Huaqiang Li,[†] Wenya Feng,[†] Xiaoxin Li, Xin Kang, Shan Yan, Menghang Chao,
Shuyuan Mo, Weiguang Sun, Yuanyuan Lu, Chunmei Chen, Jianping Wang,* Hucheng
Zhu,* and Yonghui Zhang*

Hubei Key Laboratory of Natural Medicinal Chemistry and Resource Evaluation, School of Pharmacy,
Tongji Medical College, Huazhong University of Science and Technology, Wuhan 430030, China

* Corresponding author Tel.: +86-27-83692892

E-mail addresses: zhangyh@mails.tjmu.edu.cn (Y.Z.); zhuhucheng@hust.edu.cn (H.Z.);
jpwang1001@163.com (J.W.).

CONTENT

General experimental procedures.	S1
Fungal Material.	S2
Fermentation and extraction.	S2
Purification.	S2
X-ray crystal structure analysis.	S4
Figure S1. X-ray crystallographic structure of 1	S5
AChE inhibitory activities evaluation.	S6
BChE inhibitory activities evaluation.	S6
Molecular docking	S7
Figure S2. HRESIMS spectrum of terreuspyridine (1).	S8
Figure S3. ¹ H spectrum of terreuspyridine (1)	S8
Figure S4. ¹³ C NMR and DEPT spectra of terreuspyridine (1)	S9
Figure S5. HSQC spectrum of terreuspyridine (1).	S9
Figure S6. ¹ H– ¹ H COSY spectrum of terreuspyridine (1).	S10
Figure S7. HMBC spectrum of terreuspyridine (1).	S10
Figure S8. NOESY spectrum of terreuspyridine (1).	S11
Figure S9. IR spectrum of terreuspyridine (1).	S11
Figure S10. UV spectrum of terreuspyridine (1) in MeOH.	S12
Figure S11. UV spectrum of terreuspyridine (1) in acetonitrile.	S12
Figure S12. Experimental ECD spectrum of terreuspyridine (1) in MeOH.	S13
Figure S13. Experimental ECD spectrum of terreuspyridine (1) in acetonitrile.	S13
Figure S14. HRESIMS spectrum of terreustoxin L (2).	S14
Figure S15. ¹ H spectrum of terreustoxin L (2).	S14
Figure S16. ¹³ C NMR and DEPT spectra of terreustoxin L (2)	S15
Figure S17. HSQC spectrum of terreustoxin L (2).	S15
Figure S18. ¹ H– ¹ H COSY spectrum of terreustoxin L (2).	S16
Figure S19. HMBC spectrum of terreustoxin L (2).	S16
Figure S20. NOESY spectrum of terreustoxin L (2).	S17
Figure S21. Partly enlarged NOESY spectrum of terreustoxin L (2).	S17
Figure S22. IR spectrum of terreustoxin L (2).	S18
Figure S23. UV spectrum of terreustoxin L (2) in MeOH.	S18
Figure S24. UV spectrum of terreustoxin L (2) in acetonitrile.	S19
Figure S25. Experimental ECD spectrum of terreustoxin L (2) in MeOH.	S19
Figure S26. Experimental ECD spectrum of terreustoxin L (2) in acetonitrile.	S20

General experimental procedures.

An X-5 microscopic melting point apparatus (Beijing Tech) was used, and the reported melting points were uncorrected. Optical rotations were recorded by an AUTOPOL IV-T Automatic polarimeter (Rudolph Research Analytical, Hackettstown, NJ, USA) in MeOH. A Perkin Elmer Lambda 35 UV spectrophotometer (Perkin Elmer, Inc., Fremont, CA, USA) was used to measure UV spectra. ECD curves and FT-IR spectra were collected by a JASCO-810 ECD spectrometer (JASCO Co., Ltd., Tokyo, Japan) and a Bruker Vertex 70 instrument (Bruker, Karlsruhe, Germany), respectively. NMR spectra were acquired on a Bruker AM-400 spectrometer (Bruker, Karlsruhe, Germany). The ^1H and ^{13}C NMR chemical shifts were referenced to the solvent or solvent impurity peaks for CD_3OD (δ_{H} 3.31 and δ_{C} 49.0) and CDCl_3 (δ_{H} 7.26 and δ_{C} 77.0). The HRMS (ESI) data of compound **1** was acquired on Bruker micrOTOF II spectrometer (Bruker, Karlsruhe, Germany) and the HRMS (ESI) data of **2** was obtained on a Thermo Fisher LTQ XL spectrometer (Thermo Fisher, Palo Alto, CA, USA), respectively. Column chromatography (CC) was performed with silica gel (80–120, 100–200, and 200–300 mesh; Qingdao Marine Chemical Inc., China), ODS (50 μm , YMC, Tokyo, Japan), and Sephadex LH-20 (GE Healthcare Bio-Sciences AB, Sweden). Semi-preparative HPLC was measured on an Agilent 1260 with dual pumps and a DAD detector by an RP- C_{18} column (5 μm , 10 \times 250 mm, Welch Ultimate XB- C_{18}). Thin-layer chromatography (TLC) was performed on silica gel 60 F₂₅₄ (Yantai Chemical Industry Research Institute, Yantai, China).

Fungal Material.

The fungus *Aspergillus terreus* was derived from the China General Microbiological Culture Collection Center (No. CGMCCC 3.15503). It was isolated from a soil sample which was collected from Penguin Island in Antarctic. The sequence data for this strain have been submitted to the DDBJ/EMBL/GenBank under accession No. MK685082. A voucher sample was preserved at the Huazhong University of Science and Technology (Wuhan, China).

Fermentation and extraction.

The fungal culture was incubated on potato dextrose agar (PDA) at 28 °C for 5 days. The seed culture was then aseptically transferred to inoculate 1 L Erlenmeyer flasks which were statically fermented for 28 days at room temperature on rice medium (54 kg). After harvesting, the rice medium was extracted with 95% ethanol to yield a crude ethanol extract, then suspended in water and extracted by EtOAc.

Purification.

The dry EtOAc extract (722 g) was separated by column chromatography on silica gel (CC, 3.0 kg, 25 cm × 70 cm) eluted with petroleum ether-ethyl acetate (50:1, 25:1, 10:1, 5:1, 2:1, 1:2, and 0:1). According to TLC monitoring, six fractions (Fr. 1–Fr. 6) were obtained. Fr. 3 (21.74 g) was chromatographed over ODS column (MeOH–H₂O, 20%–80%) resulting in 6 subfractions (Fr. 3.1–Fr. 3.6). Fr. 3.3 (1.44 g) was subjected to Sephadex LH-20 column (CH₂Cl₂–MeOH, 1:1) to produce five parts (Fr. 3.3.1–Fr. 3.3.5). Fr. 3.3.2 (1.14 g) was purified by semipreparative HPLC (MeCN–H₂O, 65:35, 2.0 mL/min) to yield a mixture (Fr. 3.3.2.3, 63.4 mg, t_R = 37.4 min). Fr. 3.3.2.3 was

further purified by semipreparative HPLC (MeOH–H₂O, 67:33, 2.0 mL/min) to obtain compound **2** (t_R = 42.1 min, 4.6 mg, 0.000637%). Fr. 5 (33.50 g) was subjected to a silica gel chromatography column (CC, 0.8 kg, 12 cm × 50 cm) eluted with CH₂Cl₂–MeOH (50:1–0:1, v/v) progressively to obtain seven major fractions (Fr. 5.1–Fr. 5.7). The fourth subfraction (Fr. 5.4, 5.30 g) was subsequently fractionated by a Sephadex LH-20 column (CH₂Cl₂–MeOH, 1:1) to get three subfractions (Fr. 5.4.1 to Fr. 5.4.3). Fr. 5.4.2 (3.21 g) was further subjected to RP-C₁₈ silica gel CC eluted with MeOH–H₂O (40:60–100:0, gradient system) to obtain six subfractions (Fr. 5.4.2.1–Fr. 5.4.2.6). Fr. 5.4.2.3 (146.5 mg) was purified by preparative HPLC (MeOH–H₂O, 60:40, 2.0 mL/min) to yield compound **1** (t_R = 35.6 min, 7.8 mg, 0.00108%).

Terreuspyridine (1): C₃₀H₃₉NO₈; colorless needle crystals; m.p. 201–202 °C; $[\alpha]_D^{25}$: +56.0 (*c* 0.1, MeOH); UV (MeOH) λ_{max} (log ϵ) = 200 (4.25) and 267 (3.66) nm; UV (Acetonitrile) λ_{max} (log ϵ) = 191 (4.57) and 267 (3.69) nm; IR (KBr) ν_{max} = 3455, 2989, 2952, 1741, 1712, 1634, 1576, 1448, 1352, 1267, 1169 cm^{–1}; ECD (MeOH) λ_{max} ($\Delta\epsilon$) = 190 (–5.7), 211 (+11.7), 257 (–1.1) and 297 (+4.9) nm; ECD (Acetonitrile) λ_{max} ($\Delta\epsilon$) = 211 (+17.5), 259 (–1.6) and 294 (+6.0) nm; HRMS (ESI) m/z [M + H]⁺ Calcd for C₃₀H₄₀NO₈, 542.2754; Found 542.2756. ¹H NMR (CD₃OD, 400 MHz): δ 8.39 (dd, 1H, J = 4.7, 1.7 Hz), 7.54 (dd, 1H, J = 7.8, 1.7 Hz), 7.17 (dd, 1H, J = 7.8, 4.7 Hz), 4.89 (d, 1H, J = 1.7 Hz), 4.35 (d, 1H, J = 1.7 Hz), 4.16 (s, 1H), 3.79 (s, 1H), 3.75 (s, 3H), 3.54 (s, 3H), 3.06 (d, 1H, J = 16.1 Hz), 3.04 (s, 1H), 2.94 (d, 1H, J = 16.1 Hz), 2.69 (dd, 1H, J = 15.0, 12.9 Hz), 2.61 (dd, 1H, J = 15.0, 3.2 Hz), 2.19 (dd, 1H, J = 12.9, 3.2 Hz), 1.75 (s, 3H), 1.59 (s, 3H), 1.53 (s, 3H), 1.41 (s, 3H), 1.19 (s, 3H), 0.97 (s, 3H). ¹³C NMR

(CD₃OD, 100 MHz): δ 210.5, 209.1, 174.5, 173.3, 164.0, 151.1, 148.4, 139.8, 129.7, 122.7, 111.3, 86.0, 83.0, 62.3, 58.5, 57.4, 53.7, 53.6, 51.8, 49.9, 46.6, 43.1, 40.1, 31.0, 29.2, 26.9, 26.0, 22.0, 18.2, 12.4.

Terreustoxin L (**2**): C₂₆H₃₆O₇; colorless powder; $[\alpha]_D^{25}$: +62.0 (*c* 0.1, MeOH); UV (MeOH) λ_{\max} (log ϵ) = 200 (3.99) nm; UV (Acetonitrile) λ_{\max} (log ϵ) = 191 (4.17) nm; IR (KBr) ν_{\max} = 3468, 2953, 1754, 1705, 1451, 1386, 1210, 1181 cm⁻¹; ECD (MeOH) λ_{\max} ($\Delta\epsilon$) = 196 (−6.7), 226 (+3.2), 263 (−0.1) and 306 (+1.2) nm; ECD (Acetonitrile) λ_{\max} ($\Delta\epsilon$) = 227 (+4.3), 262 (−0.1) and 306 (+1.8) nm; HRMS (ESI) *m/z* [M + Na]⁺ Calcd for C₂₆H₃₆O₇Na, 483.23587; Found 483.23518. ¹H NMR (CDCl₃, 400 MHz): δ 5.07 (d, 1H, *J* = 2.0 Hz), 5.02 (d, 1H, *J* = 2.0 Hz), 4.99 (q, 1H, *J* = 6.2 Hz), 4.53 (m, 1H), 3.63 (s, 3H), 2.85 (m, 1H), 2.80 (m, 1H), 2.57 (dd, 1H, *J* = 15.7, 3.3 Hz), 2.50 (dd, 1H, *J* = 15.1, 4.0 Hz), 2.36 (dd, 1H, *J* = 15.1, 2.4 Hz), 2.25 (ddd, 1H, *J* = 15.0, 4.3, 2.7 Hz), 2.04 (ddd, 1H, *J* = 12.8, 6.2, 2.7 Hz), 1.85 (s, 3H), 1.70 (s, 3H), 1.49 (s, 3H), 1.42 (s, 3H), 1.37 (d, 1H, *J* = 6.2 Hz), 1.22 (m, 1H), 1.17 (m, 1H), 1.15 (s, 3H), 1.12 (m, 1H). ¹³C NMR (CDCl₃, 100 MHz): δ 215.3, 203.3, 171.8, 167.5, 145.1, 113.4, 76.9, 69.0, 68.9, 55.8, 53.9, 52.3, 52.2, 48.9, 43.6, 41.7, 41.2, 37.2, 34.0, 28.5, 25.8, 25.0, 23.9, 21.0, 16.7, 15.0.

X-ray crystal structure analysis.

The crystals of compound **1** was obtained in MeOH (two drops of H₂O) by the solvent vapor diffusion method. A suitable needle crystal of **1** was analyzed on a Rigaku XtaLAB PRO MM007HF. ShelXL was used to analyze the structure solution program. The data were collected and processed using CrysAlisPro. The structures were solved

by direct methods using Olex2 software, and the non-hydrogen atoms were located from the trial structure and then refined anisotropically with SHELXL-2014 using a full-matrix least squares procedure. The crystallographic data for **1** (deposition No. CCDC 1983893) has been deposited in the Cambridge Crystallographic Data Centre.

Crystal Data for terreuspyridine (1): (C₃₀H₃₉NO₈)₂·(CH₃OH)₂·H₂O, *M* = 1165.34, *a* = 15.81020(10) Å, *b* = 8.462 Å, *c* = 23.48090(10) Å, *α* = 90°, *β* = 108.0520(10)°, *γ* = 90°, *V* = 2986.78(3) Å³, *T* = 293(2) K, space group *C*2, *Z* = 2, *μ* (Cu Kα) = 0.787 mm⁻¹, density (calcd) is 1.296 g/cm³, 32707 reflections collected, 5793 independent reflections (*R*_{int} = 0.0263) were used in all calculations. The final *R*₁ was 0.0286 and *wR*₂ was 0.0761 (*I* > 2σ(*I*)). Flack parameter was 0.01(4).

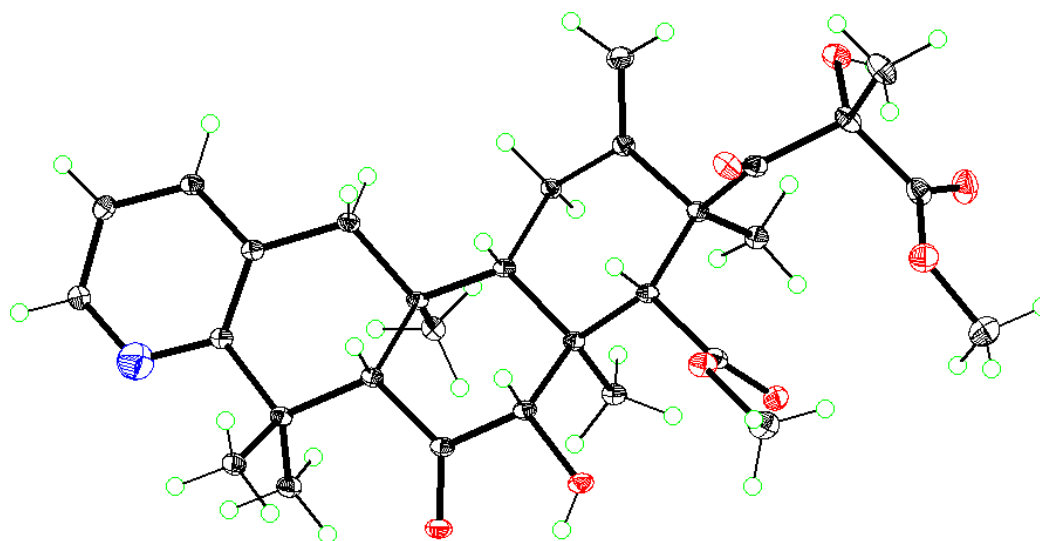


Figure S1. X-ray crystallographic structure of **1** (displacement ellipsoids are drawn at the 30% probability level).

AChE inhibitory activities evaluation.

The AChE inhibitory activity of **1** and **2** was performed by Ellman's method.^[1,2] Rivastigmine was used as positive control. The tests were performed in a sodium phosphate buffer (100 mM, pH 7.8) at 25 °C, and the reactions including buffer (126 μ L), DTNB [5,5'-dithiobis (2-nitrobenzoic acid)] (0.01 M, 50 μ L), enzyme (2 μ L), and 2 μ L of solutions containing different concentrations of **1** and **2** were incubated for 30 min. The reactions were initiated by the addition of acetylthiocholine (20 μ L, 0.075 M), and the hydrolytic activity of the acetylthiocholine was assessed by the formation of yellow-colored 5-thio-2-nitrobenzoate anions at 406 nm. Then, the assays were accomplished in triplicate using a 96-well microplate reader. The inhibition rate of AchE was calculated by the formula $[(A_0 - A_1)/A_0] \times 100$, where A_0 is the absorbance of the blank and A_1 is the absorbance observed using each concentration of **1** and **2**.^[3]

[1] Ellman, G., Courtney, K., Andres J., *et al. Biochem. Pharmacol.*, 1961, 7, 88-95.

[2] Rhee, I., Meent, M., Ingkaninan, K., *et al. J. Chromatogr. A*, 2001, 915, 217-223.

[3] Qi, C., Zhou, Q., Gao, W., *et al. Phytochemistry*. 2019, 165, 112041.

BChE inhibitory activities evaluation.

The inhibitory activity of compounds against BChE in vitro was measured using the modified Ellman's method^[1]. Briefly, 40 μ L different concentration of the tested compounds in PBS buffer (pH 7.4) and 20 μ L butyrylcholinesterase (BChE, final concentration 0.02 U/mL) were added and pre-incubated for 15 min at room temperature. The reaction mixture was then incubated for 10 min at 37 °C, after which 20 μ L 5,5'-Dithiobis-(2-nitrobenzoic acid) (DTNB, 5 mM) and 20 μ L acetylthiocholine iodide (ATCh, 10 mM) were added. The activity was determined by measuring the absorbance at 405 nm. Each concentration was done in triplicate, and IC₅₀ values were calculated graphically according to the logarithmic concentration inhibition curves (Graphpad Prism 7.0). Rivastigmine was used as a standard inhibitor.²

[1] Ellman, G., Courtney, K., Andres J., *et al. Biochem. Pharmacol.*, 1961, 7, 88-95.

[2] Damijan, K., Nicolas C., Anja P., *et al. Eur. J Med. Chem.*, **2018**, 156, 598-617.

Molecular docking

Molecular docking was performed to investigate the binding mode of compound X with butyrylcholinesterase (BChE) using Discovery Studio 4.0 (DS 4.0, Accelrys Co., Ltd., US) software. The crystal structures of soman-aged BChE (PDB ID: 4b0p) were obtained from the protein data bank for docking simulations.^[1] Molecules were built with Chemdraw and optimized at DS 4.0. LigandFit and CDOCKER docking programs implemented in DS 4.0 were used in this study. The best-scoring pose as judged by the Cdocker Interaction energy score was chosen to visual analysis using PyMOL software.^[2]

[1] Wandhammer M., De Koning M., Van Grol M., *et al. Chemi. Biol. Interact.*, 2013, 203, 19-23.

[2] Zeng Y., Cao R., Zhang T., *et al. Eur. J. Med. Chem.*, 2015, 97, 19-31.

Figure S2. HRESIMS spectrum of terreuspyridine (**1**).

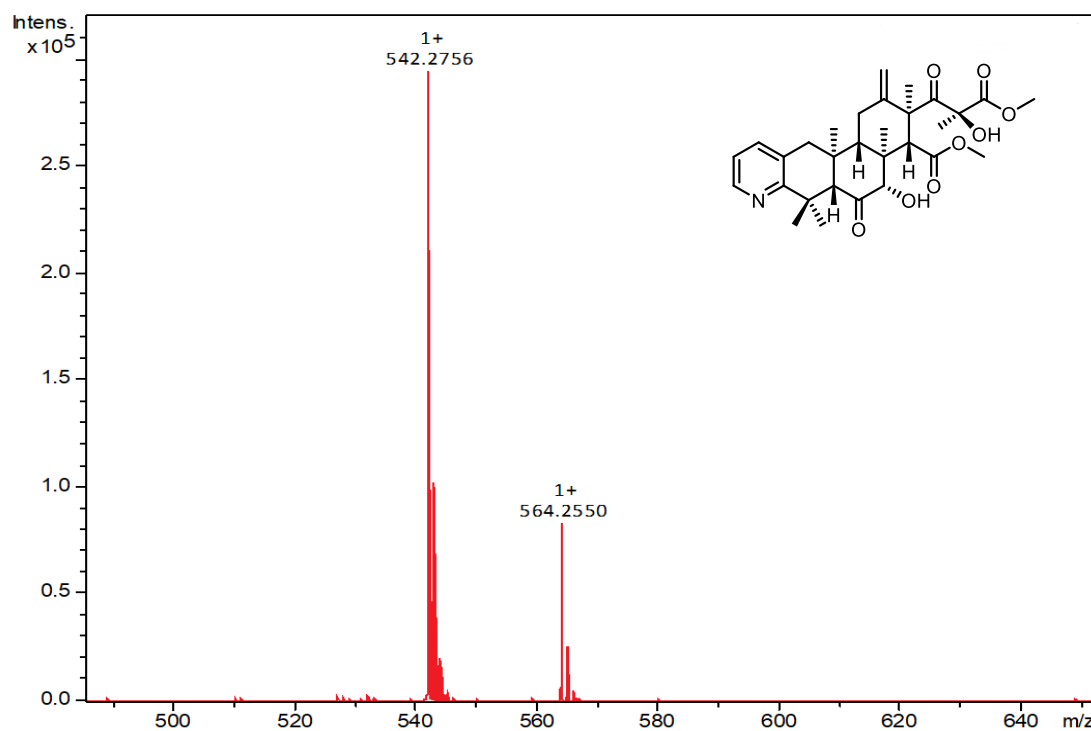


Figure S3. ¹H spectrum of terreuspyridine (**1**) (400 MHz, CD₃OD).

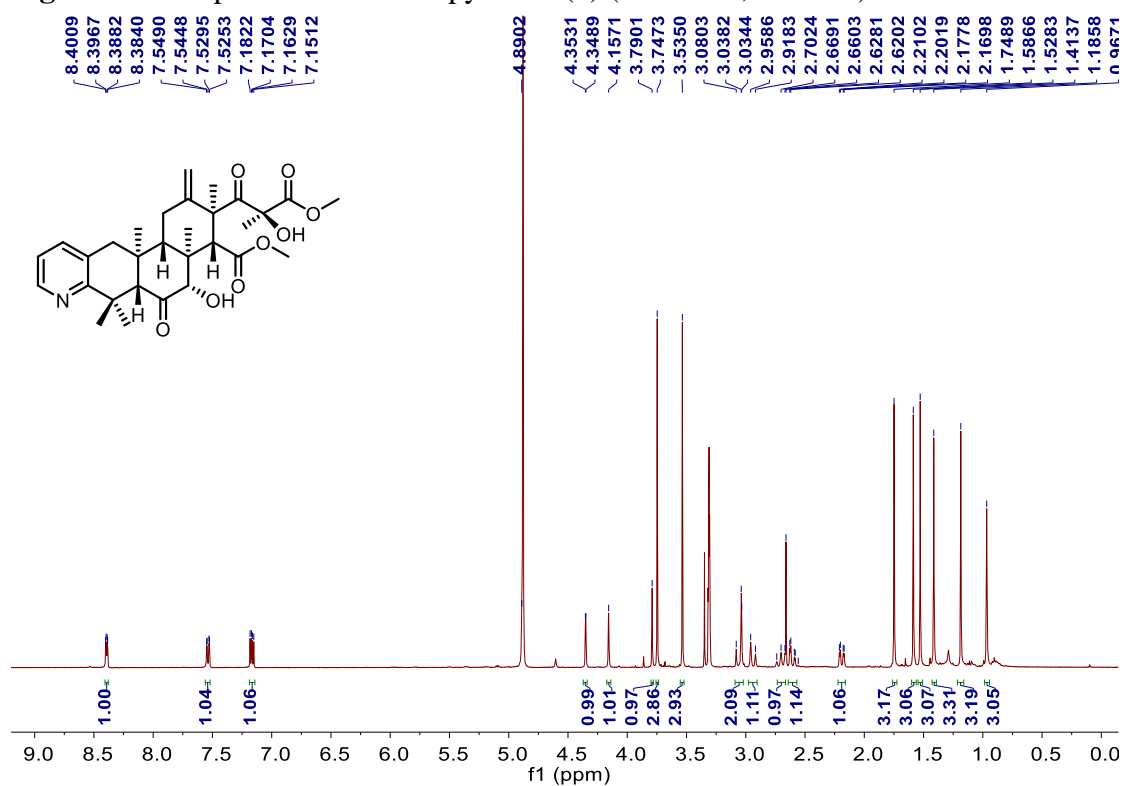


Figure S4. ^{13}C NMR and DEPT spectra of terreuspyridine (**1**) (100 MHz, CD_3OD).

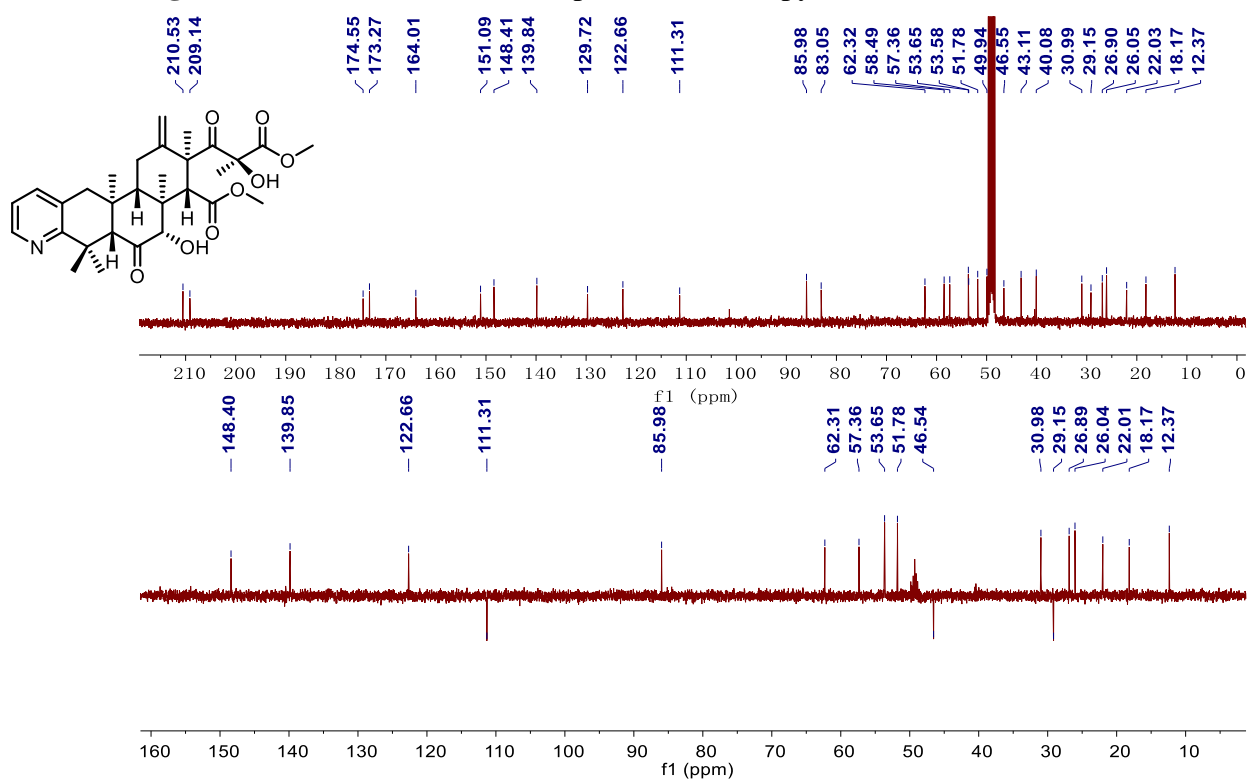


Figure S5. HSQC spectrum of terreuspyridine (**1**).

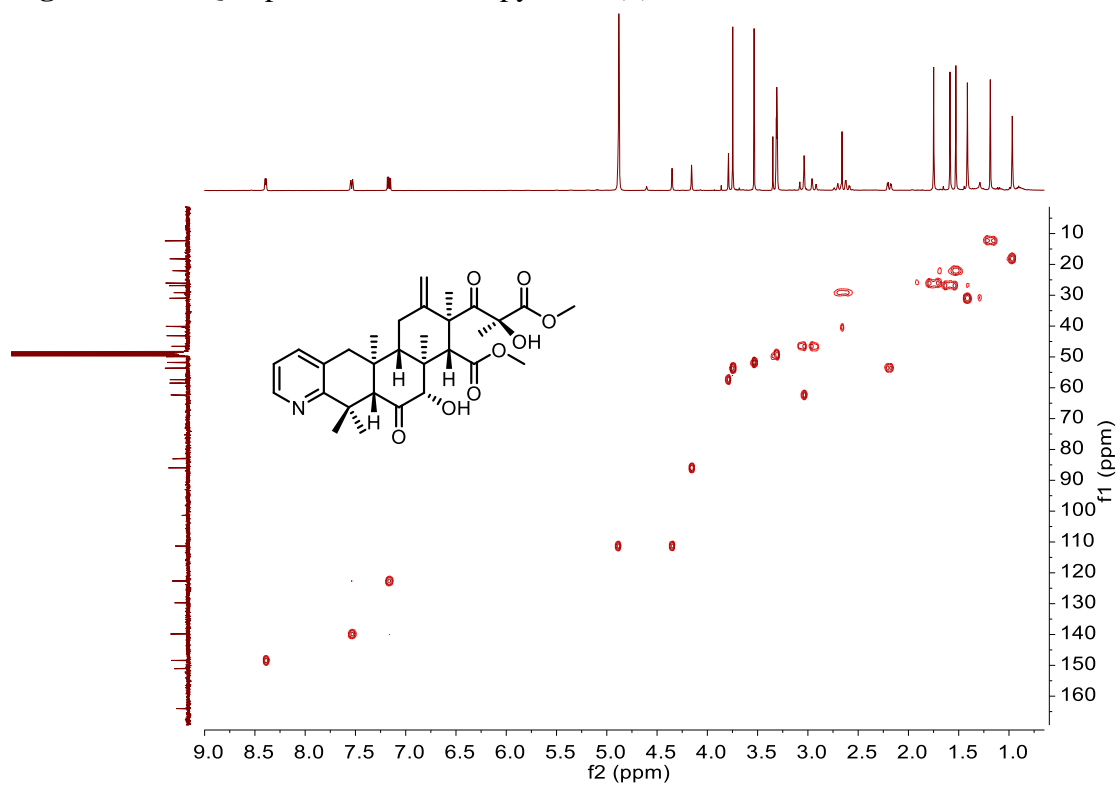


Figure S6. ^1H - ^1H COSY spectrum of terreuspyridine (**1**).

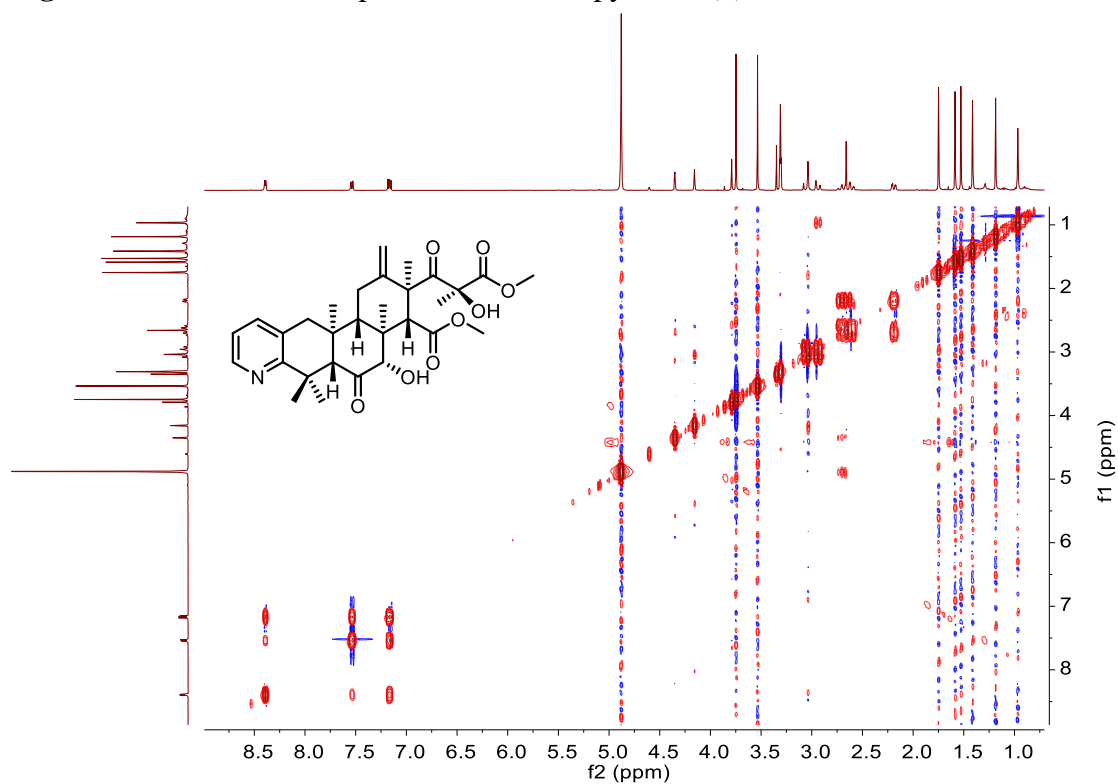


Figure S7. HMBC spectrum of terreuspyridine (**1**).

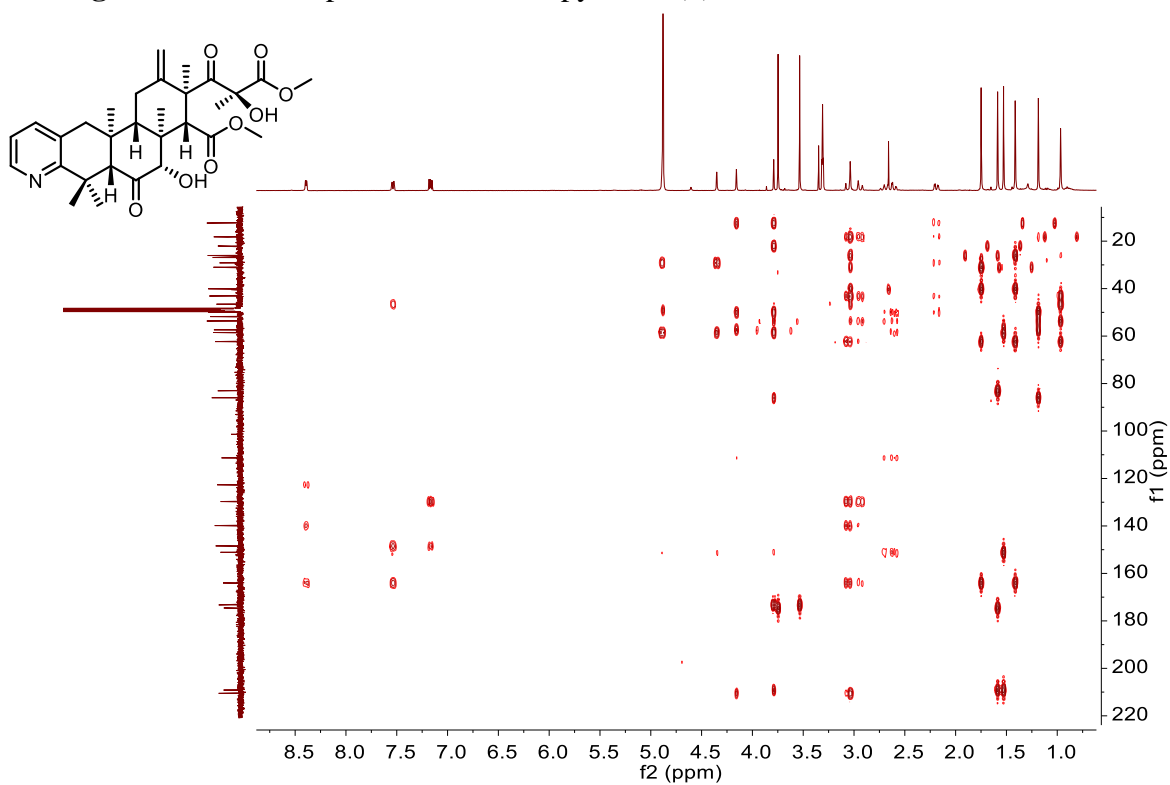


Figure S8. NOESY spectrum of terreuspyridine (**1**).

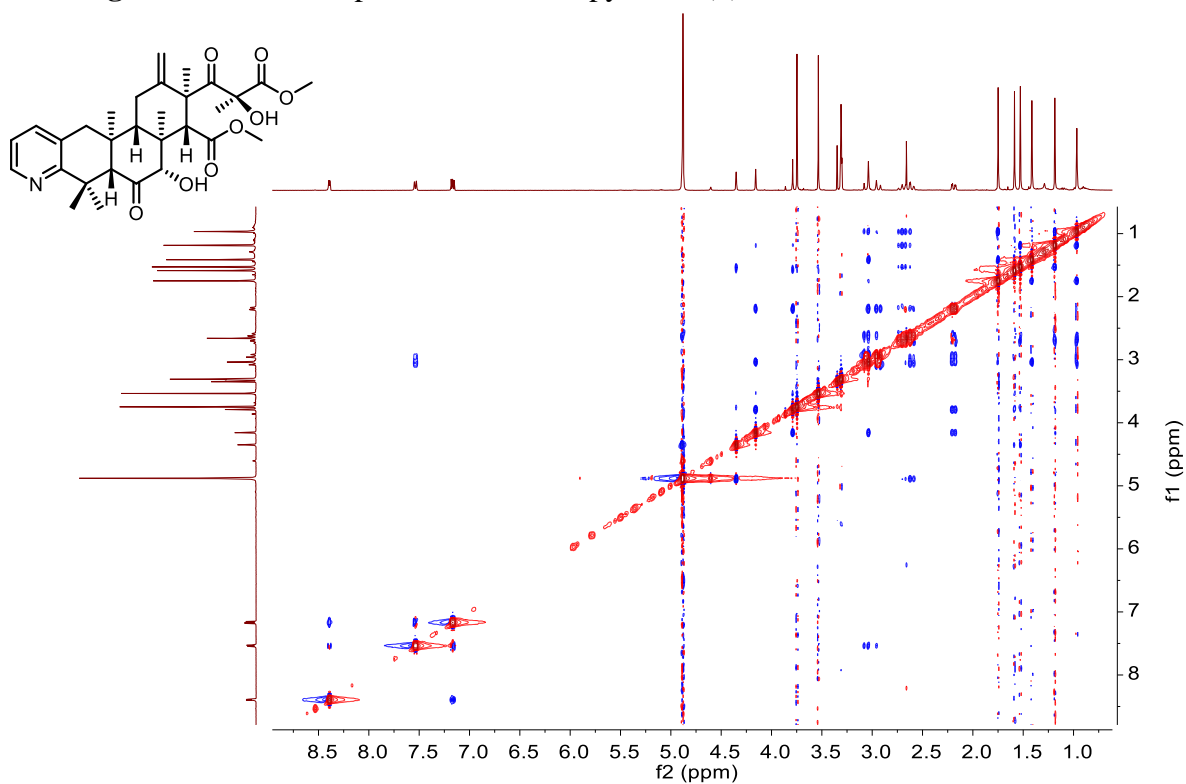


Figure S9. IR spectrum of terreuspyridine (**1**).

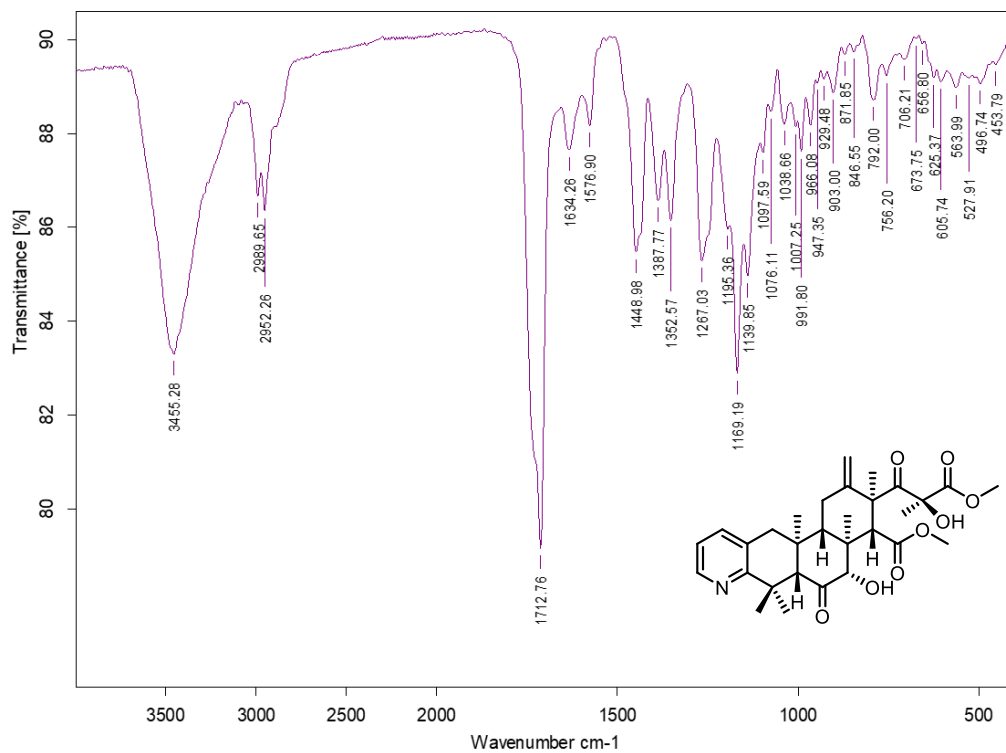


Figure S10. UV spectrum of terreuspyridine (**1**) in MeOH.

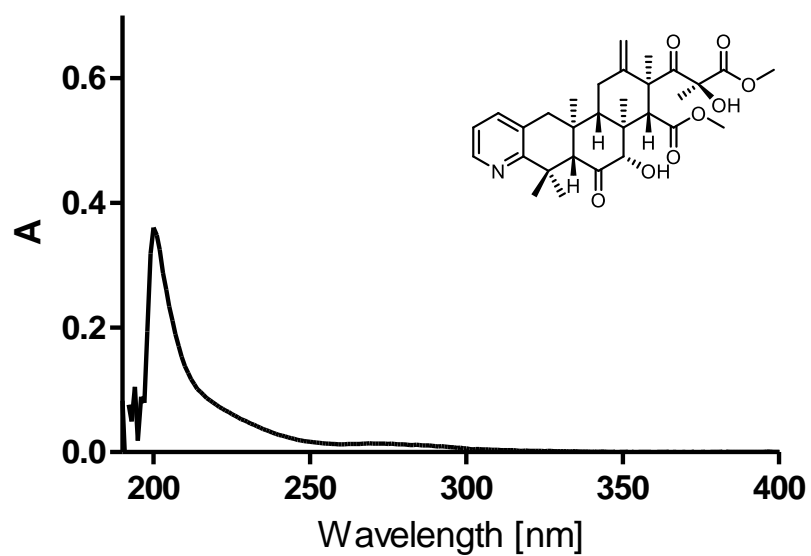


Figure S11. UV spectrum of terreuspyridine (**1**) in acetonitrile.

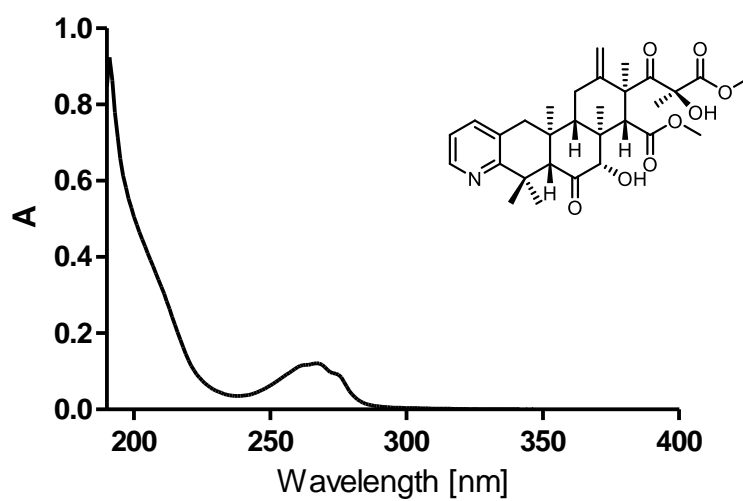


Figure S12. Experimental ECD spectrum of terreuspyridine (**1**) in MeOH.

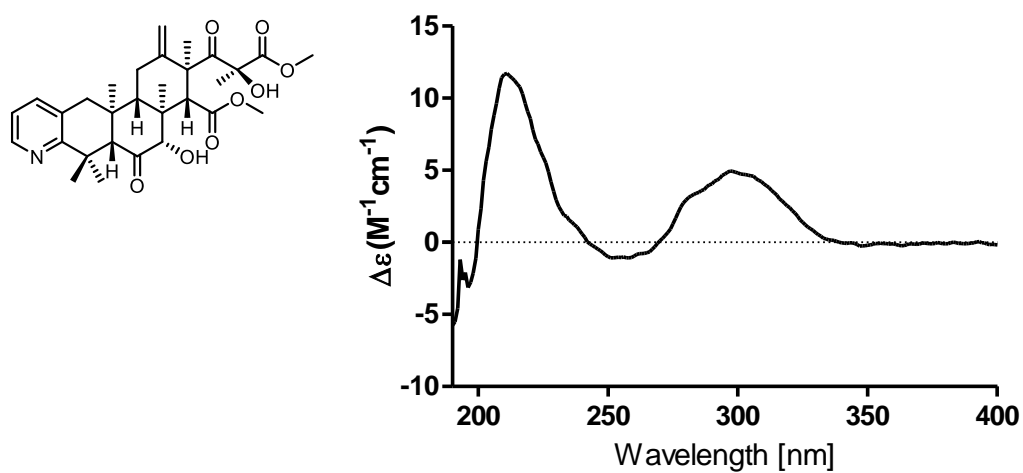


Figure S13. Experimental ECD spectrum of terreuspyridine (**1**) in acetonitrile.

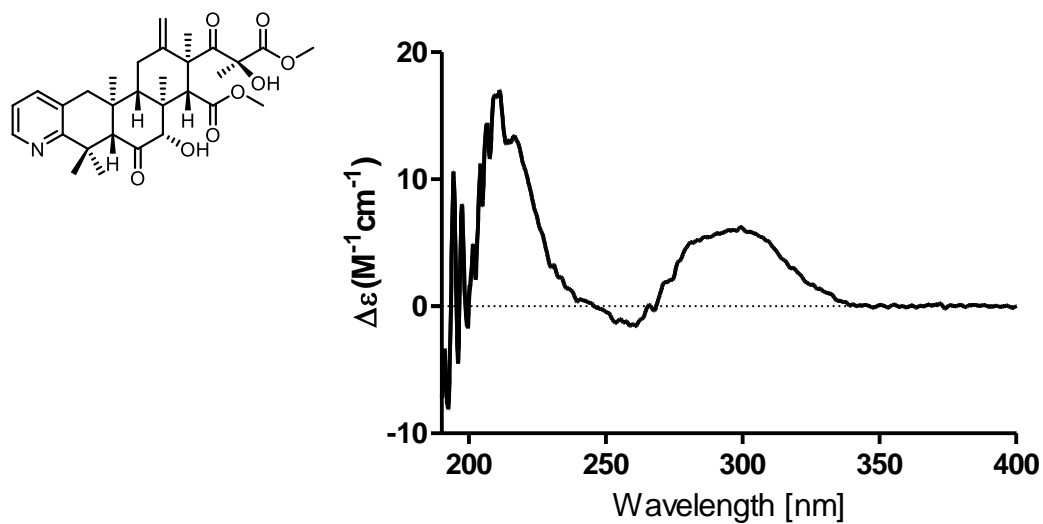


Figure S14. HRESIMS spectrum of terreustoxin L (**2**).

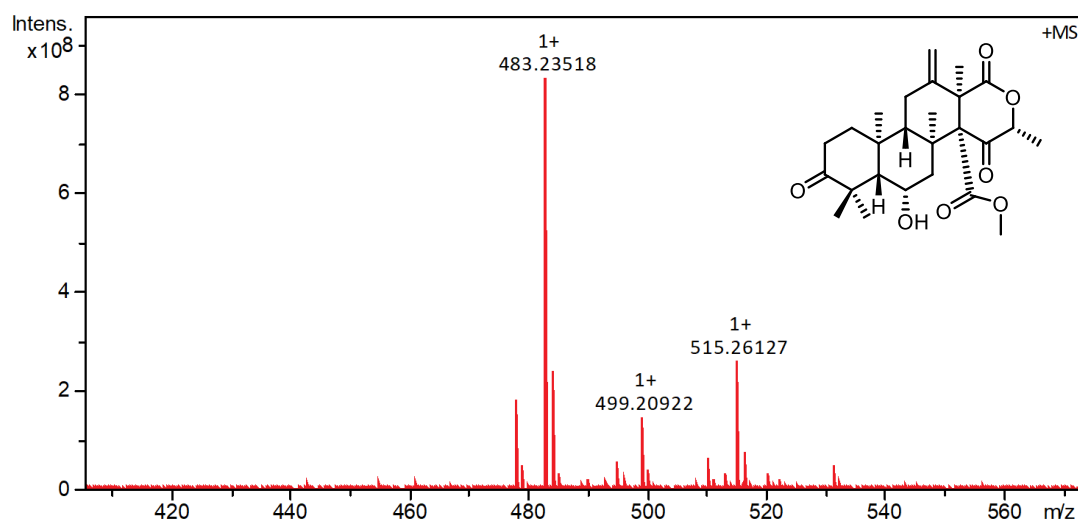


Figure S15. ¹H spectrum of terreustoxin L (**2**) (400 MHz, CDCl₃).

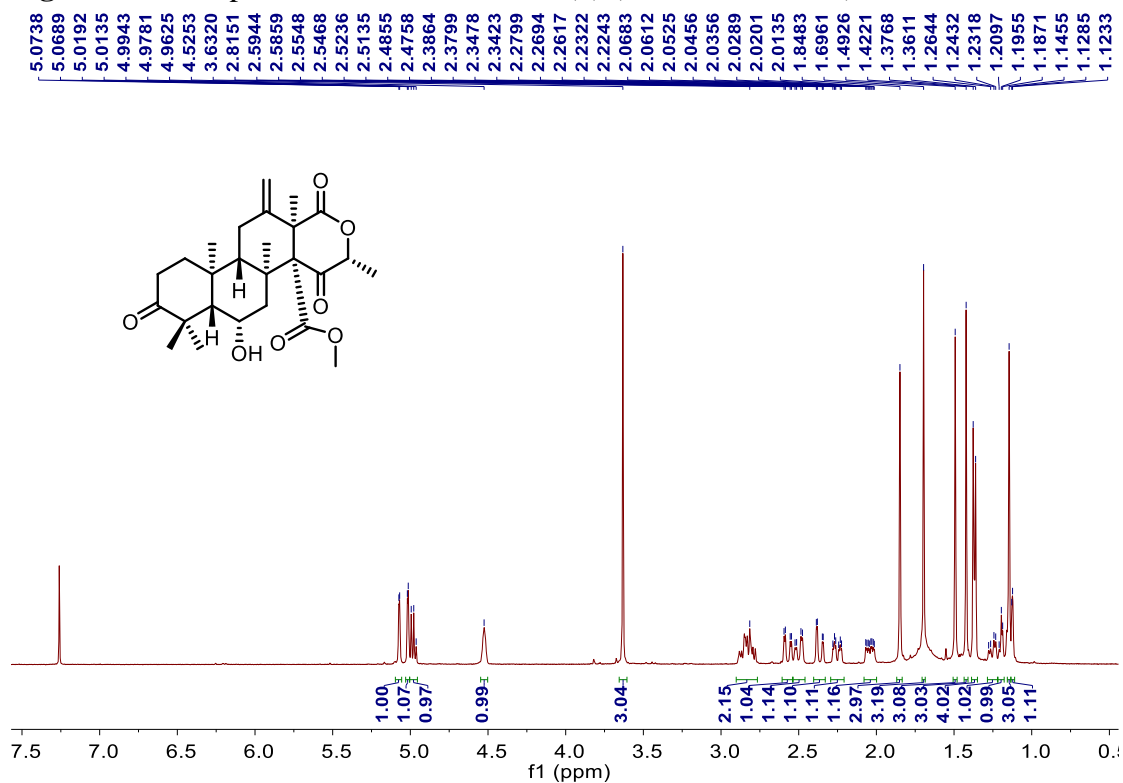


Figure S16. ^{13}C NMR and DEPT spectra of terreustoxin L (**2**) (100 MHz, CDCl_3).

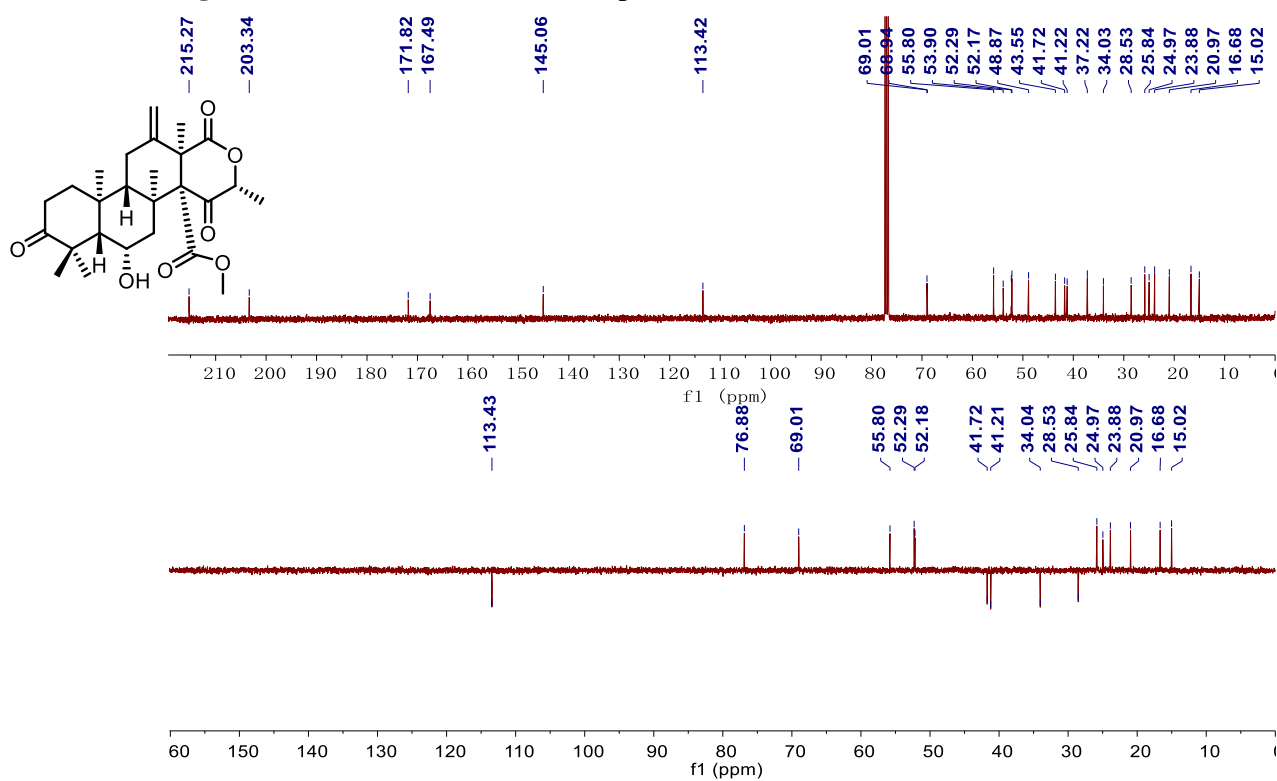


Figure S17. HSQC spectrum of terreustoxin L (**2**).

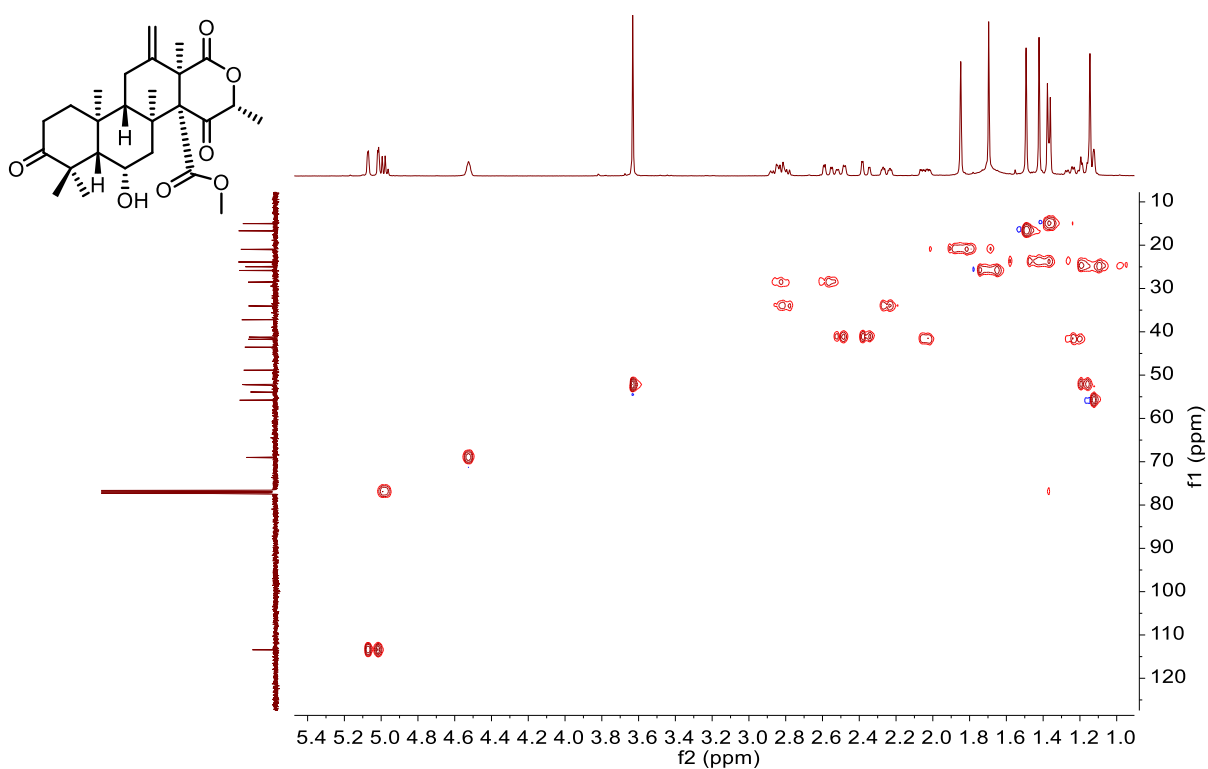


Figure S18. ^1H – ^1H COSY spectrum of terreustoxin L (**2**).

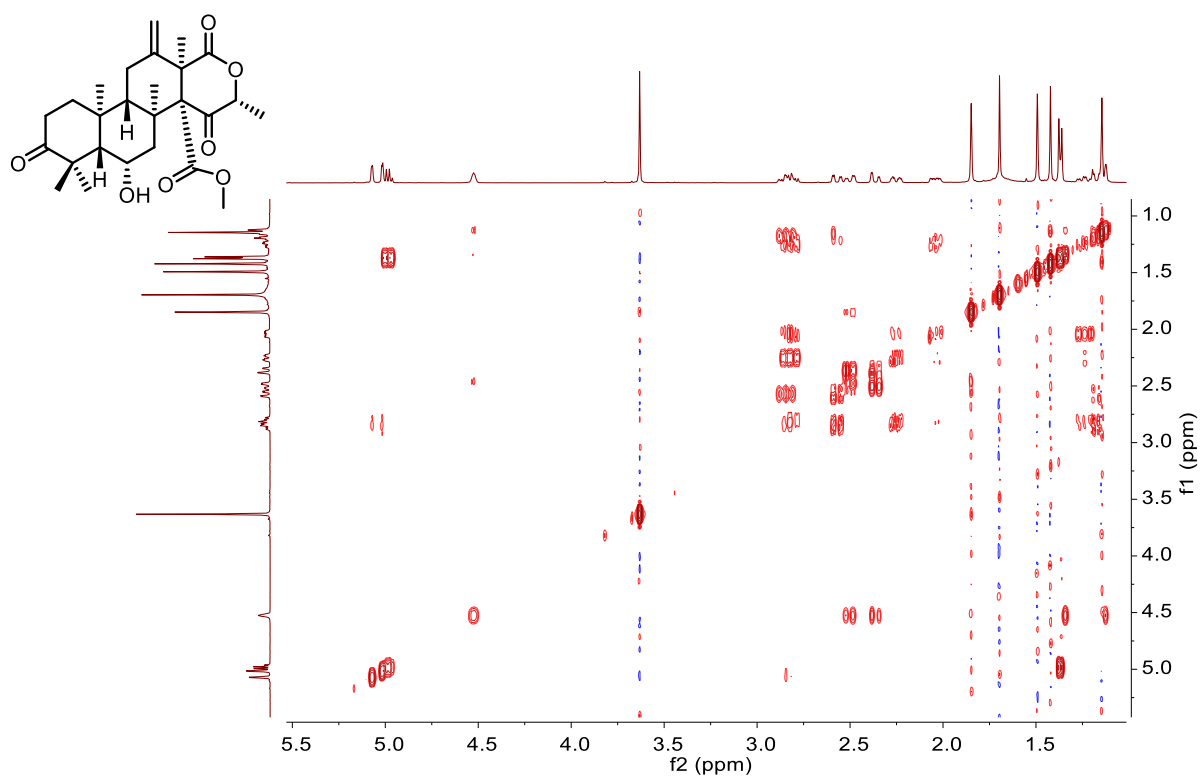


Figure S19. HMBC spectrum of terreustoxin L (2).

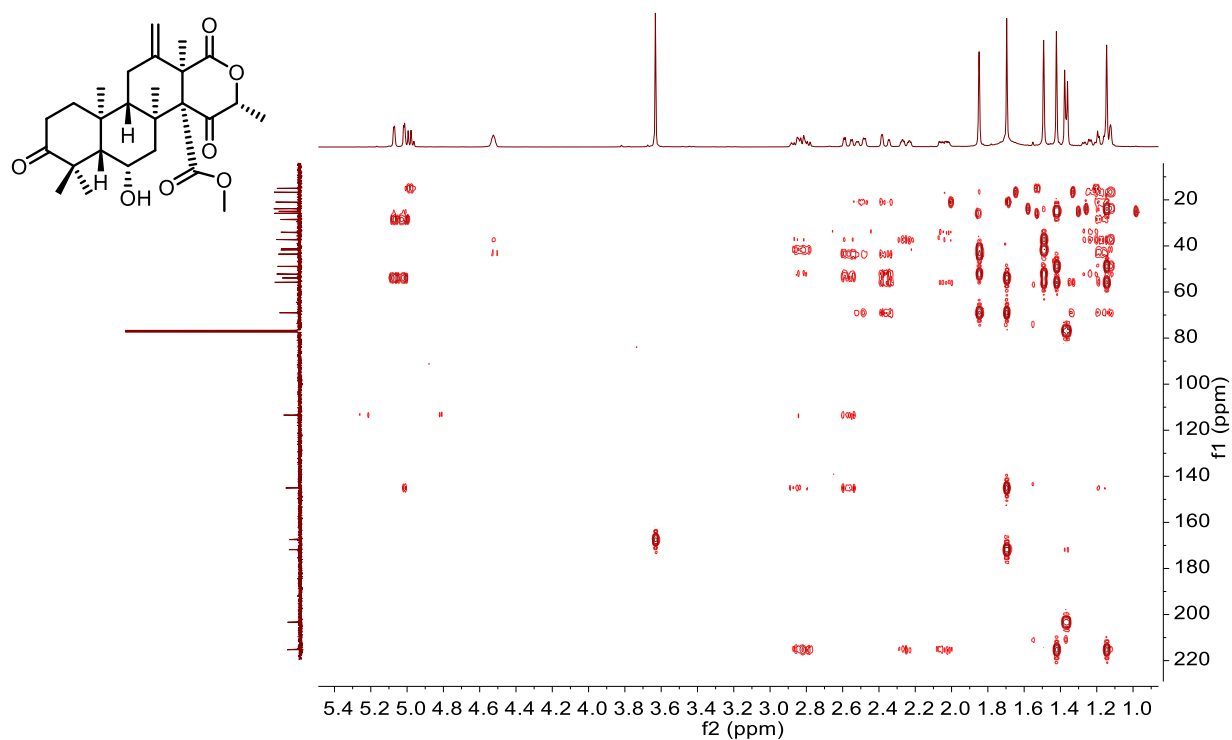


Figure S20. NOESY spectrum of terreustoxin L (**2**).

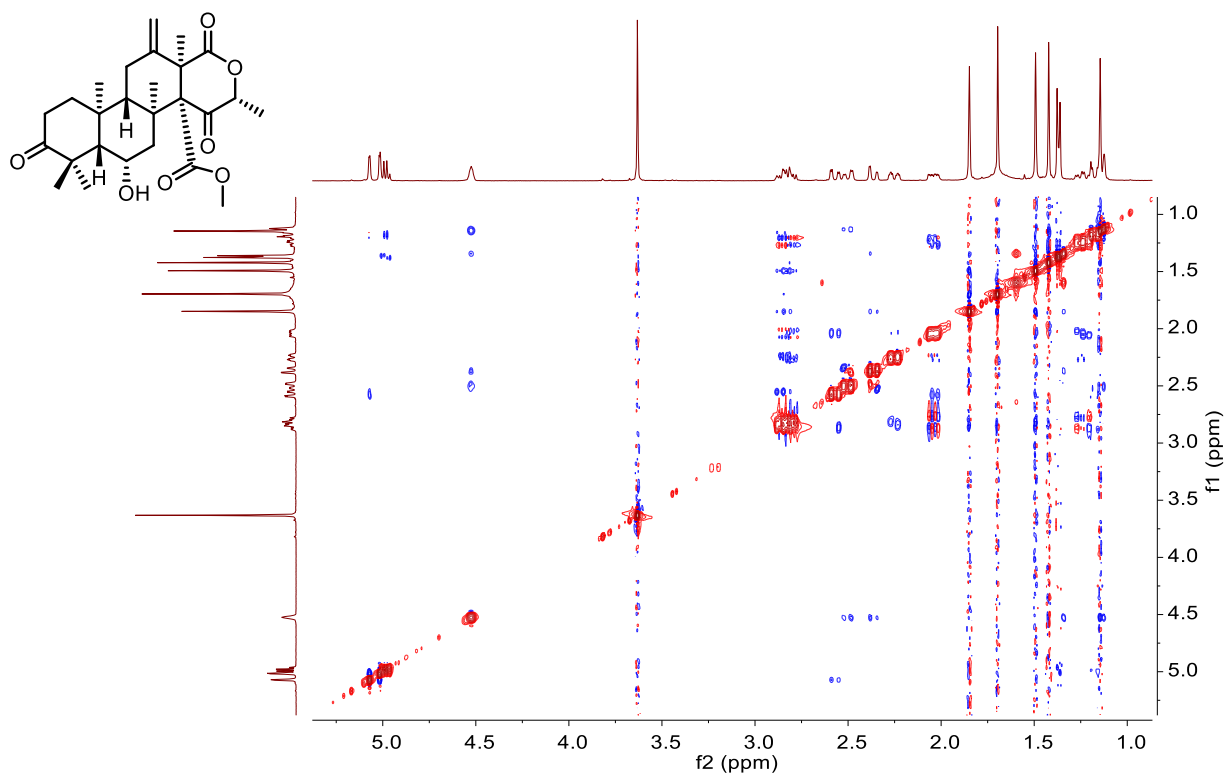


Figure S21. Partly enlarged NOESY spectrum of terreustoxin L (**2**).

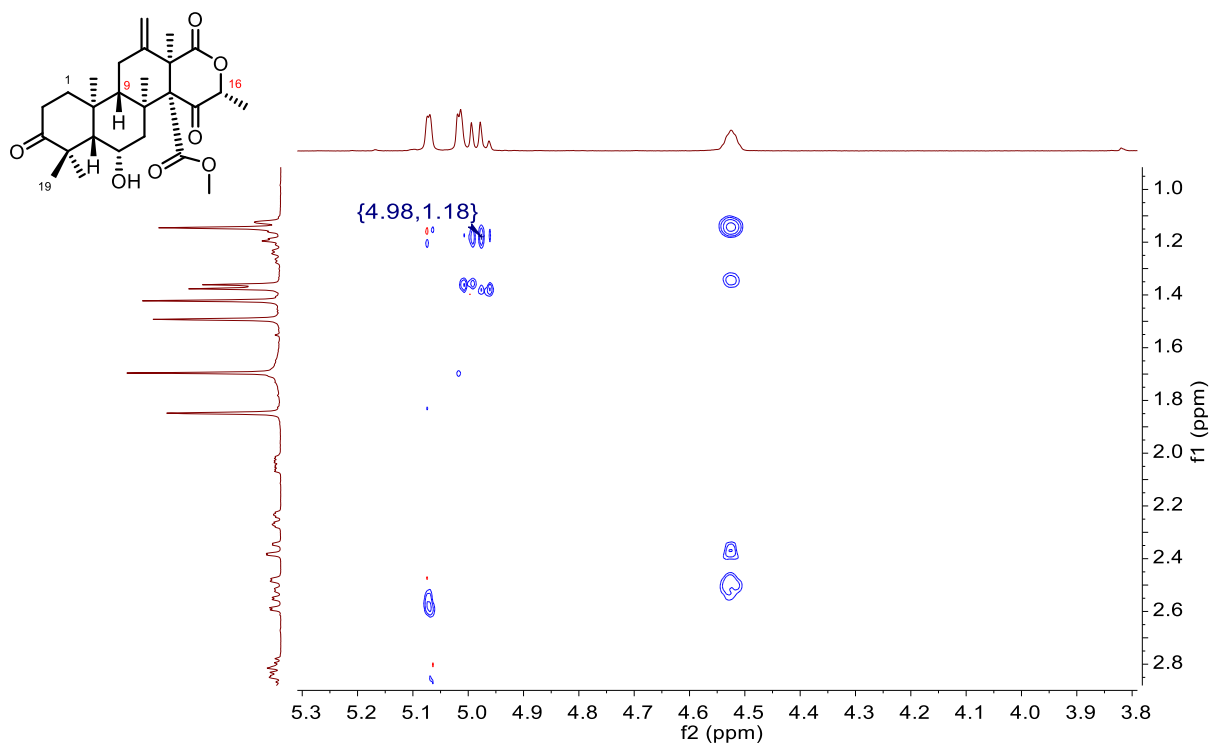


Figure S22. IR spectrum of terreustoxin L (**2**).

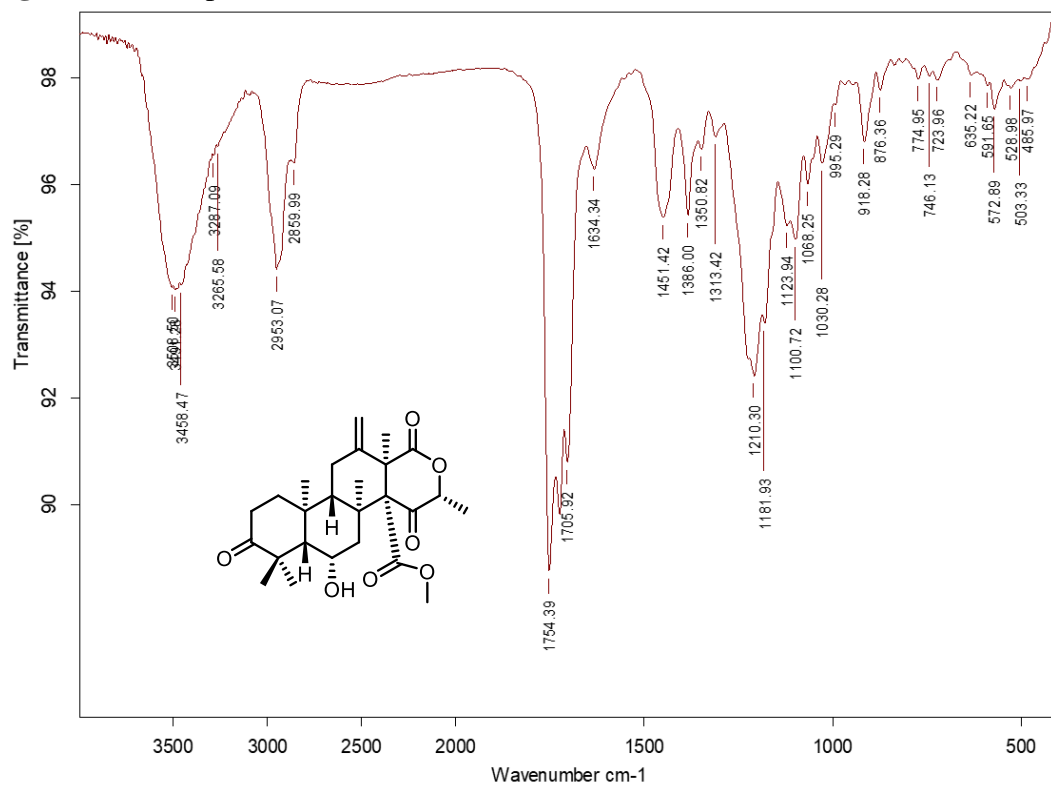


Figure S23. UV spectrum of terreustoxin L (**2**) in MeOH.

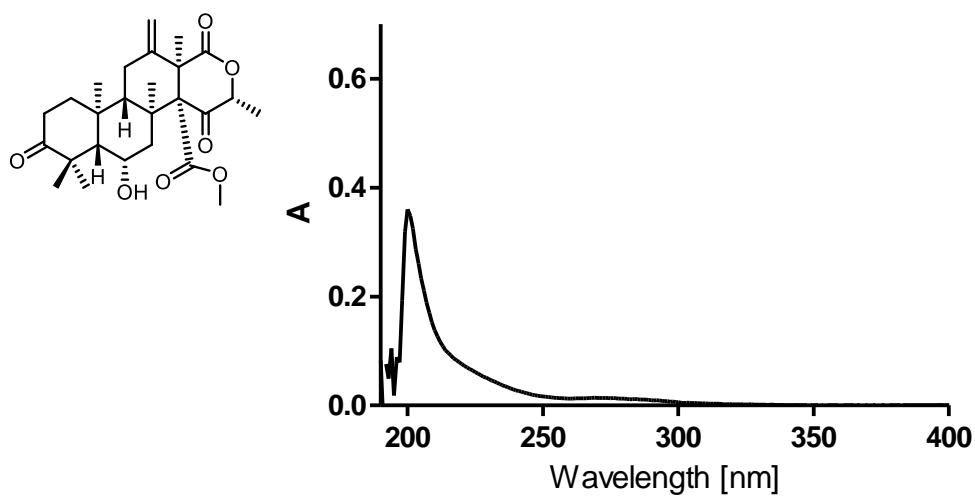


Figure S24. UV spectrum of terreustoxin L (**2**) in acetonitrile.

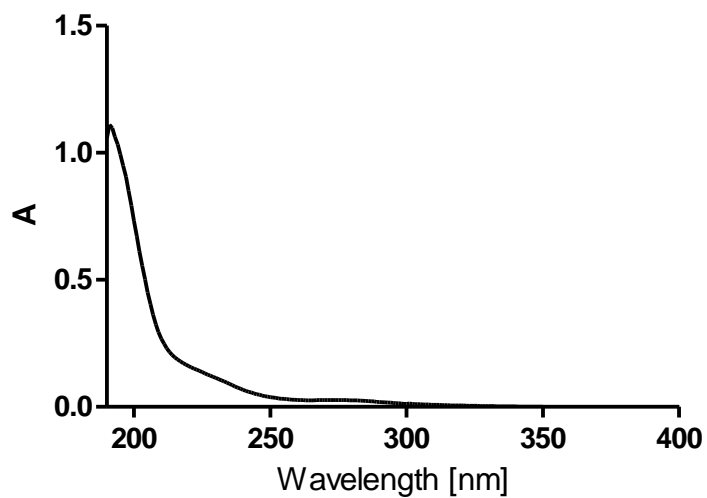


Figure S25. Experimental ECD spectrum of terreustoxin L (**2**) in MeOH.

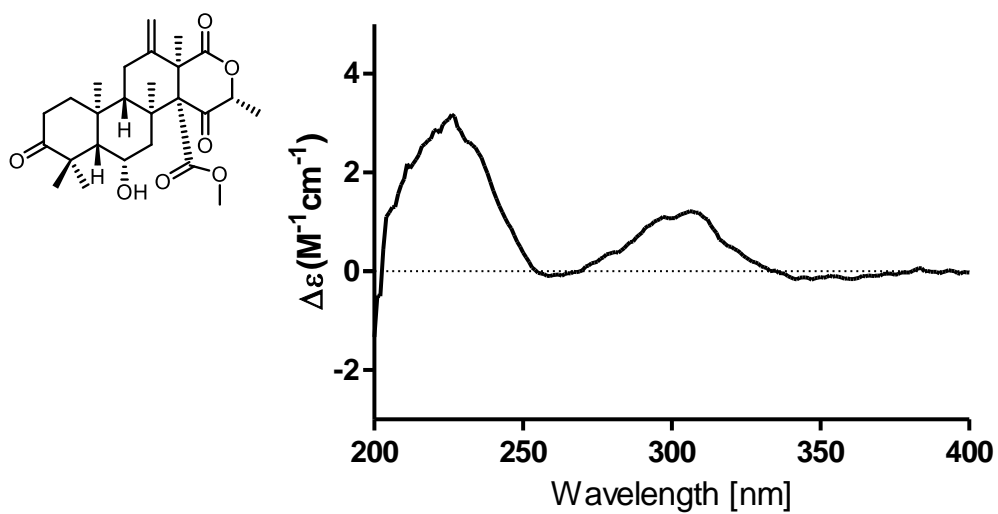


Figure S26. Experimental ECD spectrum of terreustoxin L (**2**) in acetonitrile.

